

# Session 1A4

## Bioelectronics and Medical Electromagnetics

<p><b>A Review of the Mechanisms of Interaction Between the Extremely Low Frequency Electromagnetic Fields and Human Biology</b></p> <p><i>H. A. Sadafi (Royal Melbourne Hospital, Australia); Z. Mehboodi (Amirkabir University, Iran); D. Sardari (Amirkabir University, Iran);</i> .....</p> <p><b>Calculating SAR in Two Models of the Human Head Exposed to Mobile Phones Radiations at 900 and 1800 MHz</b></p> <p><i>S. Khalatbari (Amirkabir University, Iran); D. Sardari (Amirkabir University, Iran); A. A. Mirzaee (Amirkabir University, Iran); H. A. Sadafi (Royal Melbourne Hospital, Australia);</i> .....</p> <p><b>Total Body Water Measured by Electromagnetic Resonant Cavity Perturbation</b></p> <p><i>D. A. Stone (University of York, UK); M. P. Robinson (University of York, UK); B. Oldroyd (University of Leeds, UK); J. Truscott (University of Leeds, UK); A. Wright (MRC Human Nutritional Centre, UK);</i></p> <p><b>Influence of Electric Field Variation on Intracellular K<sup>+</sup> Ion Variations and Its Implication on Electrochemical Treatment</b></p> <p><i>H. B. Kim (Solco Biomedical Institute, Korea); S. B. Sim (Catholic University, Korea); S. Y. Ahn (Solco Biomedical Institute, Korea); W. Chang (China-Japan Hospitality Hospital, China); J.-H. Li (China-Japan Hospitality Hospital, China); Y.-L. Xin (China-Japan Hospitality Hospital, China);</i> .....</p> <p><b>Qualitative Analysis of Human Semen Using Microwaves</b></p> <p><i>A. Lonappan (Cochin University of Science and Technology, India); A. V. Praveen Kumar (Cochin University of Science and Technology, India); G. Bindu (Cochin University of Science and Technology, India); V. Thomas (Cochin University of Science and Technology, India); K. T. Mathew (Cochin University of Science and Technology, India);</i> .....</p> <p><b>Microwave Thermotherapy — Technical and Clinical Aspects</b></p> <p><i>J. Vrba (Czech Technical University, Czech Republic); L. Oppl (Czech Technical University, Czech Republic); J. H. Trefna (Czech Technical University, Czech Republic); T. Drizdal (Czech Technical University, Czech Republic); R. Zajicek (Czech Technical University, Czech Republic); J. Kvěch (Institute of Radiation Oncology, Czech Republic); J. Kubeš (Institute of Radiation Oncology, Czech Republic);</i> .....</p> <p><b>Relative Absorption of Electromagnetic Energy in Adjacent Tissues</b></p> <p><i>Y. V. Narayana (ANITS Engineering College, India); G. N. Devi (55-1-26, J.R. Nagar, Venkojipalem, India); G. S. N. Raju (AU College of Engineering, India);</i> .....</p> <p><b>Detection and Identification of Bio-medical Materials Possessing Chirality Using the Mueller Matrix</b></p> <p><i>E. Bahar (University of Nebraska-Lincoln, USA);</i> .....</p> <p><b>Co-design Planar Antenna for “UWB”</b></p> <p><i>T.-P. Vuong (Institute National Polytechnique de Grenoble, France); Y. Duroc (Institut National Polytechnique de Grenoble, France); S. Tedjini (Institut National Polytechnique de Grenoble, France); G. Fontgalland (LEMA de l’Universidade Federal de Campina Grande, Brazil);</i> .....</p>	<p>178</p> <p>183</p> <p>189</p> <p>190</p> <p>191</p> <p>196</p> <p>197</p> <p>198</p> <p>199</p>
---	--

# A Review of the Mechanisms of Interaction Between the Extremely Low Frequency Electromagnetic Fields and Human Biology

H. A. Sadafi

Royal Melbourne Hospital, Australia

Zh. Mehboodi and D. Sardari

Amirkabir University, Iran

**Abstract**—Studies of the biological effects and any health related consequences of extremely low frequency (ELF) electromagnetic fields (EMF) have been going on for over half a century however with contradictory outcomes. Hence, it is now necessary to stress on standardizing the EMF-health research experiment procedures in order to enable such experiments become replicable and results comparable. In 1998, a review of several of the ELF EMF human biological interaction mechanisms regarding field intensities and frequencies was presented to the Australian Radiation Laboratory of Commonwealth Department of Community Services and Health in 1988 by Andrew W. Wood. Wood's 1988 assertion of the importance of understanding the interaction mechanisms did not alter even after a decade when the NIEHS RAPID (<http://www.niehs.nih.gov/>) gathering of world experts produced their statement, in which quoted, there have been experiments on possible mechanism/s in support or refutation of the various proposals however none were replicated. Valberg (Valberg et al., 1997) also summed up some but failed to include all the claimed proposed mechanisms at the time. This paper is to present a complete list of the allegedly possible interaction mechanisms to date.

This paper will also report on an academic research on computer modeling of biological effects of ELF EMF using one of the proposed mechanisms. The research reported here has generally aimed at modeling the proposals using computer. The initial phase of this effort has concentrated on Ca effect as the number of publications referencing that was considerable. Calcium is a key element in the biological performance of every organ in the human body. Thus it deemed imperative to study the effect of EMF on Ca channels of a living cell.

Furthermore, considerations for setting standards in EMF experimental research protocols are recommended. Developing a standard protocol allows results of future experiments to be comparable; and, the chance of replicability in EMF-health improve, which this aspect has indisputably been absent in EMF research projects thus far. Replication is desirable mainly because it eliminates bias, artifact and systematic errors. Replication is almost impossible in the case of epidemiological studies however in experimentation is possible if the details are specified in full. To authenticate any effect of MF, it is not satisfactory to present experimental results without reporting the experimental settings in their entirety.

## 1. Introduction

Allegations of the biological effects and health hazards of extremely low frequency (ELF) electromagnetic fields (EMF) have been debated for over fifty years. The epidemiological and experimental studies and clarification of conclusions of both research methods have been contradictory. Hence, stipulations have arisen for standardizing EMF-health research experiment procedures so that results of various experiments can be replicated and compared. This paper is to present a list of interaction mechanisms suggested thus far followed by a discussion on setting standard protocols in EMF experimental research. Using a standard protocol allows outcomes of experiments become comparable and replicable. The replicability attribute has undeniably been missing in EMF research projects to date [35].

## 2. Introducing the Proposed Interaction Mechanisms

Non-ionising radiations are those EMF with frequencies less than  $2 \times 10^{16}$  Hz. They can be grouped into: (i) frequencies over 1 GHz e. g., microwave, infrared and visible light; (ii) frequencies over 3 kHz but below 1 GHz e. g., those in communication systems; and, (iii) frequencies less than 3 kHz known as extremely low frequency or ELF.

The higher frequency exposure can cause dielectric heating by enforcing intra-molecular friction via vibrating momentum increase in water molecules as happens in a kitchen microwave cooking oven. Radiation in this

domain can primarily affect the human superficially e.g., skin, cranium, eyes etc and the heat generated can subsequently move deeper onto the body and effectively heat all the internal human organs. Radiation in the GHz range, e.g., mobile phone handsets, antenna and towers' exposure can cause a heating effect penetrating more inside the human body. In the ELF range ( $< 3$  kHz) for instance. when one is exposed to power-line frequencies and/or home appliances, the effects are not yet well clarified. In other words, the jury is still out on what the interaction mechanism is. Unlike the higher frequency radiations stated above, the electric and magnetic fields in the ELF range can be considered de-coupled. The electric component may barely diffuse in the human body. A widespread observation is via skin hair and only for high flux EMF. But, magnetic component may well penetrate the body nearly un-attenuated.

A review [41] of some of the ELF EMF human biological interaction mechanisms with respect to field intensities and frequencies was presented to the Australian Radiation Laboratory of Commonwealth Department of Community Services and Health in 1988. Wood's 1988 affirmation of the importance of understanding the interaction mechanisms did not alter even after a decade years when the NIEHS RAPID [27] gathering of world experts released their report, in which cited, there have been experiments on possible mechanism/s in support or refutation of the various proposals<sup>3</sup> however none were replicated. The interaction mechanisms proposed to date are:

- (1) **Magnetite;**
- (2) **Free radical;**
- (3) **Cell membrane;**
- (4) **Cell nuclei;**
- (5) **Heat shock proteins;**
- (6) **Resonance;**
- (7) **Blood-brain barrier;**
- (8) **Spatial summation;**
- (9) **Field induction;**
- (10) **Energy; and,**
- (11) **Corona.**

Describing all the above require a book to be written. However, we will endeavour to introduce these in layman terms briefly in the presentation. The suggested references in support and/or refutation and for better understanding each of the proposed mechanisms are as listed below [35].

**Magnetite:** Kirschvink et al. [2001], Phillips [1996] and NIEHS [1997].

**Free radical:** Valberg et al. [1997], Adair [1994] and NIEHS [1997].

**Cell membrane:** Miles [1969], Cotman and McGaugh [1980], McLeod [1995], Kavaliers et al. [1996], Adey [1981], Blackman et al. [1988], Wood [1988], Ueno [1996], Manni et al. [2002] and Szabo et al. [2001].

**Cell nuclei:** Lai and Singh [1997], Goodman and Blank [2002], Adair [1998], Ruiz-Gmez et al. [2002], Yomori et al. [2002] and Blank and Goodman [1998].

**Heat shock proteins:** Zryd et al. [2000].

**Resonance:** Blackman et al. [1985], Liboff et al. [1987], Lednev [1991], NIEHS [1997], Prato et al. [1996], Prato et al. [1997], Hendee et al. [1996] and Prato et al. [2000].

**Blood-brain barrier:** Andreassi [1995], Salford et al. [1994] and Lai [1992].

**Spatial summation:** Valberg et al., [1997] and Astumian et al. [1995].

**Field induction:** Gailey et al. [1997], Dimbylow [1998], Baraton and Hutzler [1996], Sagan [1996] and Kaune et al. [2002].

**Energy:** Valberg et al. [1997].

**Corona:** Fews et al. [1999], Hopwood [1992], Wood [1993].

Any experimental design to authenticate our theoretical model needs to be replicable. Replication is desirable mainly because it eliminates bias, artifact and systematic errors<sup>4</sup>. Replication is almost impossible in the case of epidemiological studies however in experimentation is possible if the details are specified in full. To substantiate any effect of MF, it is not adequate to present experimental results without reporting the experimental settings in their entirety.

A research has begun by our team using computer simulation of the proposed mechanisms starting with modeling the effect of ELF EMF on the calcium channels. The research project team preparing this paper has also aimed at modeling the proposals using computer. The initial phase of this study concentrated on Ca effect.

Calcium is a crucial element in the biological functioning of every organ in human body. Thus it is important to study the effect of EMF on Ca channels of a living cell.

### 3. Replication in EMF Research

Replication in EMF research is advantageous since it eradicates bias, artefact and systematic errors [35]. Replication is almost impossible in the case of epidemiological studies but in laboratory experimentation is achievable if the details are specified completely. To validate any biological effect of EMF, it is inadequate to present experimental results without reporting the settings fully. This would make certain the effects are replicable. A proper EMF replication necessitates applying excellent quality assurance measures to ensure matching exposure parameters [34]. These include the human biological endpoint of interest, field characteristics, exposure timing, physical dimensions of the exposure (local or whole body), field strength, DC or AC (sinusoidal or pulsating) frequency, harmonics, field alignment, field direction (linear vs. polarised), instrumentation, laboratory temperature, air-conditioning, light quantity, quality and intensity, background and environmental EMF, time of day, subject's history of exposure, subject's prior to experiment exposure, subject's adaptability to environmental factors, food intake and many others. Obviously, one has limited control over the subject's individual biological condition prior to the experiment [35].

Range of some of the parameters listed above may be controlled using correctly planned, designed and executed protocols. In planning a laboratory research project on the human health effects of EMF, biological measures chosen for the study need to be relevant.

### 4. Results and Discussion

The ELF bioelectromagnetics biological effects research has entrapped the scientists and the public in a maze since 1960's; no one has yet rescued the concerned community by provision of replicable proof [35]. Besides, a synthesis of the above-listed mechanisms may have to be considered if reasonable in an endeavor to formulate an indisputable interaction mechanism theory verifiable by experimental work.

This area of science is widely accepted as an area of controversial results. The proposed interaction mechanisms were: Magnetite; Free radical; Cell membrane; Cell nuclei; Heat shock proteins; Resonance; Blood-brain barrier; *Spatial summation*; *Field induction*; *Energy*; and, *Corona*. Acceptance or rejection of the proposals is impossible due to lack of independently replicable experiment. The parameters to be considered in a replication include the biological endpoint, field characteristics, strength, signal waveform, frequency, harmonics, alignment, direction, exposure timing, physical dimensions, instrumentation, laboratory temperature, air-conditioning, light quantity, quality and intensity, background and environmental EMF, time of day, subject's history of exposure, subject's prior to experiment exposure, subject's adaptability to environmental factors, food intake and many others. Obviously, one has limited control over the subject's individual biological condition prior to the experiment.

### 5. Conclusions

None of the alleged interaction mechanisms were proven with replication. Hence, it was concluded that, there was vividly a need for future experimental research in this field using a standard set of experimental research protocols.

Finally, experimental design efforts for testing the interaction mechanism/s theories in our research group are currently tending to focus on protein folding and Ca channels which are slow biological processes. Any experimental design to verify our theoretical model must be replicable. A replication necessitates applying excellent quality assurance measures to match exposure parameters and conditions.

### REFERENCES

1. Adair, RK., "Constraints of thermal noise on the effects of weak 60 Hz magnetic fields acting on biological magnetite," *Proc Natl Acad Sci*, No. 91, 2925–2929, USA, 2004.
2. Adair, RK., "Extremely low frequency fields do not interact directly with DNA," *Bioelectromagnetics*, No. 19, 136–138, 1998.
3. Adey, WR., "Tissue interactions with nonionizing electromagnetic fields," *Physiol Rev* 61, 435–514, 1981.
4. Andreassi, JL., "Psychophysiology: human behavior and physiological response," *Lawrence Erlbaum*, NJ, 1995.

5. Astumian, RD., JC. Weaver, and RK. Adair, "Rectification and signal averaging of weak electrical fields by biological cells," *Proc Natl Acad Sci*, No. 92, 3740–3, USA, 1995.
6. Baraton, P and B. Hutzler, "Magnetically induced currents in the human body," *IEC Technology Trend Assessment. Geneva. International Electrotechnical Commission.*
7. Blackman, CF., SG. Benane, DE. House, and WT. Joines, "A role for the magnetic field in the radiation-induced efflux of calcium ions from brain tissue in vitro," *Bioelectromagnetics*, No. 6, 327–337, 1985.
8. Blackman, CF., SG. Benane, DJ. Elliot, DE. House, and MM. Pollock, "Influence of electromagnetic fields on the efflux of calcium ions from brain tissue in vitro: a three-model analysis consistent with the frequency response up to 510 Hz," *Bioelectromagnetics*, No. 9, 215–227, 1988.
9. Blank, M and R. Goodman, "Do electromagnetic fields interact directly with DNA," *Bioelectromagnetics*, No. 19, 136–138, 1998.
10. Cotman, CW and JL. McGaugh, "Behavioural neuroscience," *An introduction. Academic Press*, New York, USA.
11. Dimbylow, PJ., "Induced current densities from low-frequency magnetic fields in a 2 mm resolution, anatomically realistic model of the body," *Phys Med Biol*, No. 43, 221–230, 1998.
12. Fews, AP., DL. Henshaw, PA. Keitch, JJ. Close, and RJ. Wilding, "Increased exposure to pollutant aerosols under high voltage powerlines," *Int J Radiat Biol*, No. 75, 1505–1521, 1999.
13. Gailey, P., A. Sastre, and RE. McGaughy, "Internal electric field produced by EMF, dosimetry, and endogenous fields," C. Portier and M. Wolfe (Eds), EMF science review symposium breakout group reports for theoretical mechanisms and in vitro research findings, Phoenix, AZ, NIEHS, 55–70, 1997.
14. Goodman, R. and M. Blank, "Insights into electromagnetic interaction mechanisms," *J Cell Physiol*, No. 192, 16–22, 2002.
15. Hendee, SP., FA. Faour, DA. Christensen, B. Patrick, CH. Durney, and DK. Blumenthal, "The effects of weak extremely low frequency magnetic field on calcium/calmodulin interactions," *Biophys J*, No. 70, 2915–2923, 1996.
16. Hopwood, A., "Natural radiation focused by powerlines," New evidence, *Electronics World & Wireless World*, November.
17. Kaune, WT., T. Dovan, RI. Kavet, DA. Savitz, and RR. Neutra, "A study of high- and low-current-configuration homes from the 1988 Denver childhood cancer study," *Bioelectromagnetics*, No. 23, 177–188, 2002.
18. Kavaliers, M., KP. Ossenkopp, FS. Prato, DG. Innes, LA. Gaba, DM. Kinsella, and TS. Perrot-Sinal, "Spatial learning in deer mice: gender differences and the effects of endogenous opioids and 60 Hz magnetic fields," *J Compar Physiol*, No. 179, 715–724, 1996.
19. Kirschvink, JL., MM. Walker, and CE. Diebel, "Magnetite-based magnetoception," *Curr Opin Neurobiol*, No. 11, 462–467, 2001.
20. Lai, H., "Research on the neurological effects of nonionizing radiation at the university of washington," *Bioelectromagnetics*, No. 13, 513–526, 1992.
21. Lai, H and NP. Singh, "Acute exposure to a 60 Hz magnetic field increases DNA strand breaks in rat brain cells," *Bioelectromagnetics*, No. 18, 156–165, 1997.
22. Lednev, VV., "Possible mechanism for the influence of weak magnetic fields on biological systems," *Bioelectromagnetics*, No. 12, 71–75, 1991.
23. Liboff, AR., SD. Smith, and BR. McLeod, "Experimental evidence for ion cyclotron. Mechanistic approaches to interaction of electric and electromagnetic fields with living systems," M. Blank and E. Findl (Eds). *Plenum Press*, New York, USA, 1987.
24. Manni, V., A. Lisi, D. Pozzi, S. Rieti, A. Serafino, L. Giuliani, and S. Grimaldi, "Effects of extremely low frequency (50 Hz) magnetic field on morphological and biochemical properties of human keratinocyte," *Bioelectromagnetics*, No. 23, 298–305, 2002.
25. McLeod, KJ., "The role of cell and tissue calcium in transducing the effects of exposure to low-frequency electromagnetic fields. In: Electromagnetic fields: biological interactions and mechanisms," M. Blank, (Ed), Washington DC, American Chemical Society, 349–365, 1995.
26. Miles, FA., *Excitable cells*, Heinemann, London, 1969.
27. NIEHS, *EMF Sci Rev Symposium*, EMF RAPID. Website Address: <http://www.niehs.nih.gov/emfrapid/html/symposium1.html/symposium2.html> and [/symposium3.html](http://www.niehs.nih.gov/emfrapid/html/symposium3.html), 1997.

28. Phillips, JB., "Magnetic navigation," *J theor Biol*, No. 180, 309–319, 1996.
29. Prato, FS., M. Kavaliers, and J.J.L. Carson, "Behavioural evidence that magnetic field effects in the land snail, *cepea nemoralis*, might not depend on magnetite or induced electric currents," *Bioelectromagnetics*, No. 17, 123–130, 1996.
30. Prato, FS., M. Kavaliers, AP. Cullen, and AW. Thomas, "Light-dependent and -independent behavioral effects of extremely low frequency magnetic fields in a land snail are consistent with a parametric resonance mechanism," *Bioelectromagnetics*, No. 18, 284–291, 1997.
31. Prato, FS., M. Kavaliers, and AW. Thomas, "Extremely low frequency magnetic fields can either increase or decrease analgesia in the land snail depending on field and light conditions," *Bioelectromagnetics*, No. 21, 287–301, 2000.
32. Ruiz-Gómez, MJ., L. de la Peña, MI. Prieto-Barcia, JM. Pastor, L. Gil, and M. Martinez-Morillo, "Influence of 1 and 25 Hz, 1.5 mT magnetic fields on antitumor drug potency in a human adenocarcinoma cell line," *Bioelectromagnetics*, No. 23, 578–585, 2002.
33. Sadafi, HA., "Human physiological effects of power frequency magnetic fields.," *M.App.Sc. Thesis*, Swinburne University of Technology, Melbourne, Australia, 1993.
34. Sadafi, HA., "Replicability in EMF research," *Progress in Electromagnetics Research Symp PIERS-1999*, Taipei, Taiwan, 1999.
35. Sadafi, HA., "Human brain effects of 50 Hz power frequency magnetic fields," *PhD Thesis*, Swinburne Univ. Australia, 2003.
36. Sagan, LA., "Electric and magnetic fields: invisible risks," *Gordon and Breach*, Amsterdam, 1996.
37. Salford, LG., A. Brun, K. Stureson, JL. Eberhardt, and BR. Persson, "Permeability of the blood-brain barrier by 915 MHz electromagnetic radiation, continuous wave and modulated at 8, 16, 50 Hz," *Microsc Res Tech*, 27, 535–542, 1994.
38. Szabo, L., MA. Rojavin, TJ. Rogers, and MC. Ziskin, "Reactions of keratinocytes to in vitro millimeter wave exposure," *Bioelectromagnetics*, No. 22, 358–364, 2001.
39. Ueno, S. and M. Iwasaka, "Magnetic nerve stimulation and effects of magnetic fields on biological, physical and chemical processes. Biological effects of magnetic and electromagnetic fields," S. Ueno (Ed)., *Plenum Press*, New York, 1996.
40. Valberg, PA., R. Kavet, and CN. Rafferty, "Can low-level 50/60 Hz electric and magnetic fields cause biological effects," *Radiat Res*, No. 148, 2–21, 1997.
41. Wood, AW., "Carcinogenic potential of extremely low frequency magnetic fields," Proc of a Workshop Held at the Australian Radiation Laboratory on May 17, 1988.
42. Wood, AW., Report on 1993 Annual Contractor's Review. EMF Update, Electricity Supply Association of Australia (ESAA) December Report, 1993.
43. Yomori, H, K. Yasunaga, C. Takahashi, A. Tanaka, S. Takashima, and M. Sekijima, "Elliptically polarized magnetic fields do not alter immediate early response gene expression levels in human glioblastoma cells," *Bioelectromagnetics*, No. 23, 89–96, 2002.
44. Zryd, J. P., DG. Schaefer, M. Ianoz, and P. Zwiackner, "Influence of 50 Hz magnetic fields on the moss *Physcomitrella patens*," 4<sup>th</sup> *European Symposium on Electromagnetic compatibility*, EMC 2000, Brugge, 2000.

# Calculating SAR in Two Models of the Human Head Exposed to Mobile Phones Radiations at 900 and 1800 MHz

S. Khalatbari<sup>1</sup>, D. Sardari<sup>1</sup>, A. A. Mirzaee<sup>1</sup>, and H. A. Sadafi<sup>2</sup>

<sup>1</sup>Amirkabir University, Iran

<sup>2</sup>Royal Melbourne Hospital, Australia

**Abstract**—Since the 1990's, use of mobile phones has augmented worldwide generating a public concern as to whether frequent utilization of such devices is unsafe. This provoked EMF researchers to find suitable techniques of assessing radiation blueprint and exposure hazards if any. Most research groups focused on two techniques: experimental measurements and finite-difference time-domain (FDTD) computations. Computation of the specific absorption rate (SAR) generated by cellular phones inside two models of the human head is presented in this paper. Two models of mobile phones were considered working at 900 and 1800 MHz bands according to the Global System for Mobile Communication. Radiated energy distributions and averaged SAR values in 1g and 10g of tissue were computed inside the models of head using FDTD. Computations were compared with a realistic head model constructed with the MRI scans. The distribution of the local SAR in the head was similar to that of the simplified head models. The maximum local SAR calculated was 53.43 W/kg and the maximum SAR(10g) was 2.96 W/kg, both for 1 W output power from the antenna. The results indicated the area of the maximum local SAR was situated in outer layer of skull, where muscle and skin were. The important parameters in absorbed energy in the head were the type of antenna, current distribution and the distance between head and antenna. The head models used for simulation proved as insignificant parameter in the calculations.

## 1. Introduction

Within only the last ten years, mobile phone usage has been rapidly spread globally. In chorus with the expanding usage, a question has been raised repeatedly as to whether frequent usage of such a device which radiates GHz electromagnetic field onto the human head is unsafe. This rapid expansion has thus pushed the research toward the necessity of finding a reliable means of analyzing mobile phone for radiation pattern performance to address the safety concerns. It is broadly accepted that mobile phones cause heating of the human organ exposed to their radiation and specifically the human head. The current exposure limits are based on Specific Absorption Rate (SAR) of the exposure heat. A SAR limit of 2 W/kg averaged over any contiguous 10g head tissue was recommended by the Council of European Union [1] for the general public. This recommendation in a way acknowledged that a simple cubical geometry used may yield calculated dosimetric quantities of conservative values corresponding to the exposure guidelines.

It has been a while since, most research groups studying biological effects of mobile phones have focused on two methods: *experimental measurements* and *finite-difference time-domain* (FDTD) computations [2-5]. While experimental measurements make use of the actual mobile phone being tested [6], there remains a question of appropriateness of representing the human head with simplified phantoms that for compliance testing include, at most, two or three tissue type materials [4, 5]. The FDTD method, on the other hand, can be questioned on its lack of a realistic anatomically heterogeneity representation of the radiation exposure of mobile phone through the human head model [7].

In the research work reported here, the authors focused on the absorption of energy in the human head from near-field radiation of wireless phones. Two models for mobile phone (half-wavelength dipole and a quarter-wavelength monopole) and two simple models for head (homogenous and multi-layer spherical) were considered. A modern method for calculating maximum SAR (10g) was introduced and the results were compared with a realistic MRI model of head [6, 7].

## 2. Numerical Method and Modeling

Two models used for the human head were spheres of 20 cm diameter. The first model was a sphere consisting entirely of material with the electric properties of brain tissue. The second model comprised three layers as illustrated in Fig. 1. The spherical model had a uniform content at its core (representing the human brain) and the core was surrounded by two spherical shells representing the skull (bone) and the muscle and skin (skin) with their respective electromagnetic properties.

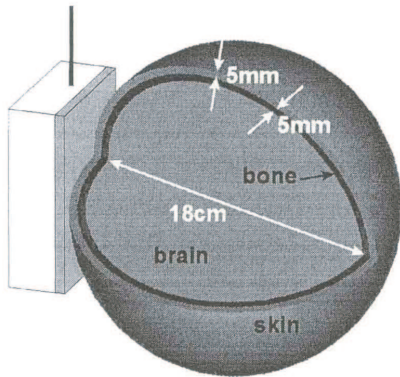


Figure 1: The model of the layered sphere.

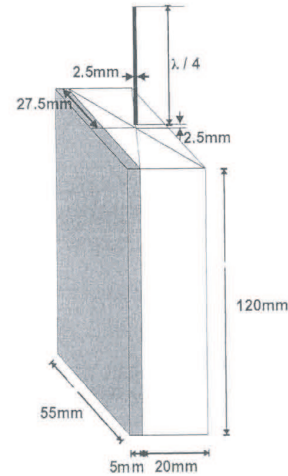


Figure 2: The model of the monopole antenna mounted on top of the metal box.

The handset has been modeled in two different ways, namely a half-wavelength dipole and a quarter-wavelength monopole both mounted on top of a metal box. The thickness of the antennas in both cases was one FDTD cell. The antennas were centered on the top surface of a conducting box with dimensions  $120 \text{ mm} \times 55 \text{ mm} \times 20 \text{ mm}$  (see Fig. 2). The face of the metal box next to the user was covered with a dielectric material of 5 mm thickness. The feeding gap of the dipole antenna was placed at a distance of 0.5 mm from the sphere. However, the feeding gap of the monopole antenna located 2 cm away from the sphere, since the minimum distance between the sphere and metal box was again 0.5 cm [4, 5, 8].

The simulation was performed at the two common telecommunication carrier frequencies of 900 MHz and 1800 MHz. The handset antenna model length was adjusted according to the wavelength in free space obviously corresponding to the frequency in use. Combinations of the cases were also investigated as detailed in Table 1. The properties of tissue material considered in the computer simulation modeling at both frequencies [3] were as tabulated in Table 2.

Table 1: Description of the cases examined.

Case	Homogeneous Sphere	Layered Sphere	900 MHz	1800 MHz	Dipole	Monopole
1	*		*		*	
2	*		*			*
3	*			*	*	
4	*			*		*
5		*	*		*	
6		*	*			*
7		*		*	*	
8		*		*		*

A software sourced from the Utah University of Technology (<http://www.fDTD.org>) was used for the simulation. The lattice for all cases was formed by a uniform rectilinear grid with a space step of 2.5 mm in all three directions. The simulation time was twenty periods of the source signal. A hard source model was positioned at the feeding gap, which had the size of one cell [3, 9–12]. The source had a sinusoidal time behavior and was switched on at the beginning of the computer run. In all simulations the output power of the antenna was 1 W. Mur's second-order absorption boundary conditions [13, 14] were used to truncate the computational domain.

The distribution of the local SAR values can be calculated directly from the electric field distribution, which results from the computer run. This was achieved using Eq. (1) as the sinusoidal source leads to a steady state electric field, numerically analogous with the same sinusoidal variation [3–6].

$$SAR = \frac{\sigma E_{\max}^2}{2\rho} \quad (1)$$

Table 2: The properties of the materials used in the simulations.

Material	900 MHz $\epsilon_r$	900 MHz $\sigma$	1800 MHz $\epsilon_r$	1800 MHz $\sigma$	Mass Density (Kg/m <sup>3</sup> )
<i>Skin</i>	39.5	0.7	38.2	0.9	1080
<b>Bone (cortical)</b>	12.5	0.17	12.0	0.29	1180
<b>Brain (Grey matter)</b>	56.8	1.1	51.8	1.5	1050
<b>Dielectric Phone Cover</b>	2.7	0.0016	2.7	0.003	-

To test the hypothesis that steady state was reached after twenty periods of the numerical source signal, the time evolution of the electric field at several points in the lattice was monitored during each computer run [3, 7, 15]. It was found that for all the cases examined, the simulation time was more than enough to arrive at steady state.

The derivation of the average SAR values needs some post-processing of the simulation results. The SAR values were averaged over 1 g and 10 g of tissue. The way averaging volume was selected was crucial for the derived average SAR distributions [3, 7, 15]; hence the averaging procedure adopted had to be clarified. The edge of each cell in the lattice was 2.5 mm which allowed for a 1 cm cube to be considered per four cells. This cube provided 1 g of tissue for a mass density of 1 g/cm<sup>3</sup>. Noting that the area of SAR (10 g) was situated outside of the skull area (in the muscle) and the size of the cube was sufficiently small. Therefore, the computation output results allowed direct calculation of the maximum SAR. Conversely, it was impossible to have a cubic volume of tissue with a mass of 10 g; and, as in the previous method a cube of 2.25 cm sides (nine cells) was considered (method 1). In this case, due to the long length of the cube and its location with different SAR specially in between skull/brain and skull/muscle, the calculations resulted in a noticeable difference with previously published studies. The process details were reviewed and checked again and found to be precise. Furthermore, two cubes were considered, 1.75 cm<sup>3</sup> (seven cells) and 2.25 cm<sup>3</sup> (nine cells) co-centered as illustrated in Fig. 3. The SAR (10 g) value was subsequently calculated considering the contribution of the smaller cube and the contribution of the cubical shell around it each with a predefined weighting coefficient using Eq. (2).

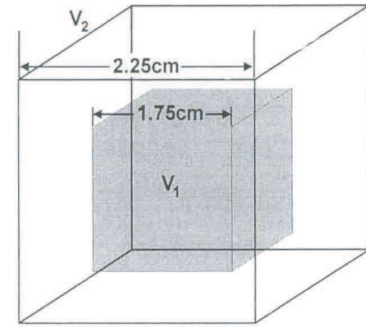


Figure 3: The cube volumes used for calculating the SAR (10 g) values.

$$SAR(10g) = \frac{\sum_{v_1} (SAR)_i m_i + \sum_{v_2-v_1} (SAR)_j m_j}{\sum_{v_1} m_i + \sum_{v_2-v_1} m_j} \quad (2)$$

where  $m_i = \rho_i \Delta V$  and  $m_j = \rho_j \Delta V \frac{10-V_1}{V_2-V_1}$  [3]. Index  $i$  refers to the lattice cells inside the inner cube and index  $j$  to those around it (method 2).

Table 3: Total absorbed power, maximum SAR(1g), maximum SAR(10g) and local SAR in the head model (antenna output power 1 W).

Case	$P_{abs}$ (W)	$SAR(1g)_{max}$ (W/kg)	$SAR(10g)_{max}$ (W/kg) (Method 1)	$SAR(10g)_{max}$ (W/kg) (Method 2)	Local $SAR_{max}$ (W/kg)
1	0.77	2.45	2.96	1.89	26.19
2	0.41	0.74	0.82	0.53	4.23
3	0.75	4.67	6.15	3.89	70.16
4	0.24	0.52	0.63	0.41	3.92
5	0.76	1.64	1.91	1.22	18.86
6	0.48	0.5	0.58	0.37	3.72
7	0.83	4.13	5.01	3.18	54.14
8	0.30	0.59	0.69	0.44	4.87

### 3. Results

Table 3 presents a summary of the total absorbed power, the maximum SAR (1 g), the SAR (10 g) and local SAR values. These results indicated that the model of the handset device played a more important role in dosimetry than the model of human head. This was evident when looked at the difference in calculated values; for instance, considering case 1 (homogeneous sphere, 900 MHz,  $\lambda/2$  dipole) with case 5 (layered sphere, 900 MHz,  $\lambda/2$  dipole) yielded smaller figures than when the case 1 was considered with case 2 (layered sphere, 900 MHz,  $\lambda/4$  monopole). As reported previously [4, 5, 8], this research confirmed that in most cases the homogeneous sphere resulted in a larger SAR values than the layered sphere. It was also apparent from the results in Table 3 that modeling the handset as a dipole yielded higher SAR values than modeling it as a monopole.

However a direct comparison between the respective pairs of cases was not possible, because it could be argued that the smaller distance of the dipole feeding gap to the head may account for the larger SAR values. So, the distance of the  $\lambda/2$  dipole was varied for case 3 (homogeneous sphere, 1800 MHz,  $\lambda/2$  dipole) to study its significance. As shown in Fig. 4, at 2 cm distance the values obtained with the  $\lambda/2$  dipole are still larger than case 4 (homogeneous sphere, 1800 MHz,  $\lambda/4$  monopole). It can be noted from Fig. 4 that the maximum local SAR doesn't fall off inversely proportional to the square of distance, as it would in the far field.

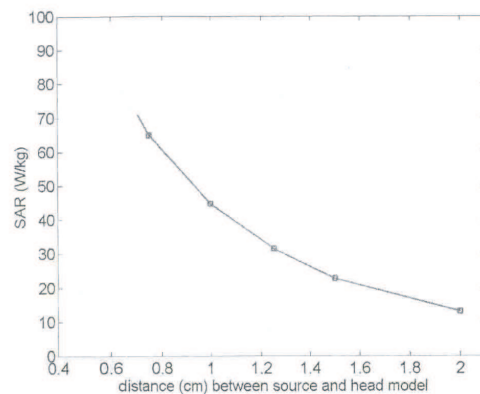


Figure 4: Variation of maximum local SAR values.

The effect of different operating frequencies was as illustrated in Fig. 5 and Fig. 6. An observation was that the SAR decreased faster in the higher frequency range as expected due to the smaller penetration depth.

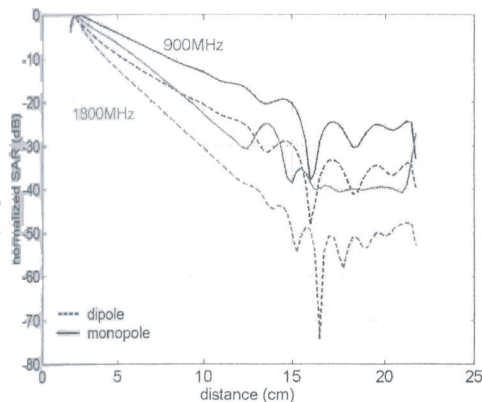


Figure 5: The profile of local SAR across the homogeneous spherical head model. The distance was measured from the point of the source closest to the head model. The SAR values were normalized to the maximum to show the effect of frequency.

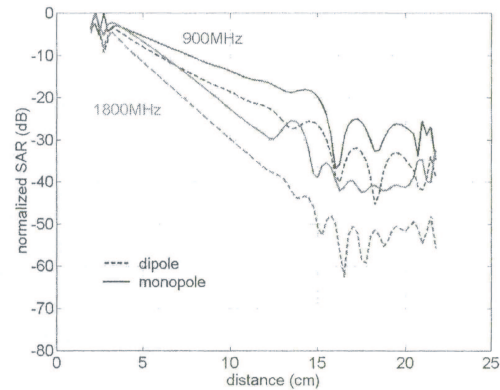


Figure 6: The profile of local SAR across the layered spherical head model. The distance was measured from the point of the source closest to the head model. The SAR values were normalized to the maximum to show the effect of frequency.

### 4. Comparison between Case Study and MRI Human Head Model

The MRI model used in this work was the Bradford University Telecommunication Research Center Tissue-classified high-resolution voxel image of a human head [6, 7]. The original resolution of the model was 0.909 mm

in the x and y direction on the axial plane and 1.480 mm in the z (vertical) direction. The phantom was re-sampled to have cubic voxels with each side of 0.25 mm length. A  $\lambda/4$  monopole on top of a metal box was used for the device model, with the source operating at 900 MHz. The distribution of the local SAR in the head (Fig. 7) was similar to that of the simplified head models. The maximum local SAR calculated was 53.43 W/kg and the maximum SAR(10 g) was 2.96 W/kg, both for 1 W output power from the antenna.

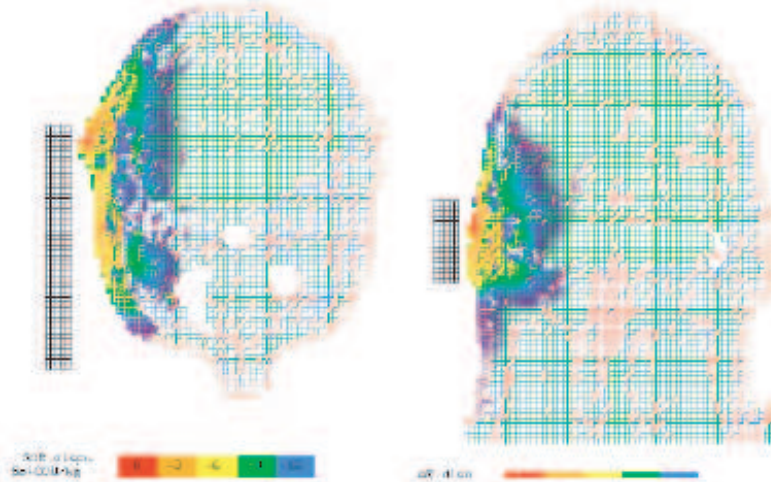


Figure 7: Distribution of the local SAR on a) the middle coronal plane and b) the middle axial plane of the MRI head model for the monopole on top of the Box operating at 900 MHz. The values are normalized to the maximum local SAR.

### 5. Discussion and Conclusions

The maximum SAR(10 g) value was higher than the basic limit of 2 W/kg SAR(10 g) over 6 minute period according to the widely adopted exposure guidelines [1]; however, the following points must be noted:

1)In the simulations, it was assumed that the device was operating continuously. Nevertheless, time-averaged power of a GSM device under real operating conditions was 1/8 of its nominal power. Therefore, for a nominal operating power of 1W the actual time-averaged output power was 0.125W [see also 3-5, 7, 8, 15].

2)The introduction of a dielectric scatterer like the human head in the vicinity of the radiating antenna alters the input impedance of the latter. In the calculations it was assumed that all the power generated and transmitted by the electronic devices to the antenna was fully radiated out; i.e., the antenna and the transmission line were completely matched. This assumption represented the worse case since only a portion of the power was radiated from the antenna.

3)It was shown that the use of a metal box model for the phone instead of a CAD model gives more conservative results, i.e., higher SAR values [6].

Although the total absorbed power in most cases was lower for 1800 MHz than for 900 MHz, the maximum SAR values are higher for the higher frequency. The distribution of SAR in the spherical head models shown as in Fig. 7, indicated that the large SAR values were restricted within a volume close to the surface of the model. In fact, in more than 94% of the head model volume the SAR was smaller than 10% of the local maximum SAR for each case (see Fig. 8).

Finally, the results demonstrated that the area of the maximum local SAR was situated in outer layer of skull, where muscle and skin were located. Since the maximum difference in dielectric properties between muscle and skull was more than other tissues, the maximum reflection happened around the boundary of the

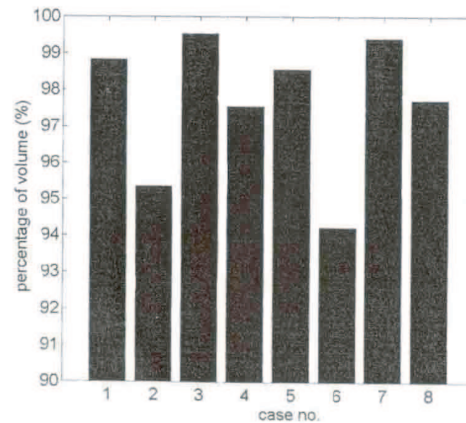


Figure 8: Percentage of volume in the spherical head models for which the local SAR has a value smaller than 10% of the maximum local SAR.

two tissues. Thus maximum absorption power was seen in this border; and, because of the skin effect, with increasing frequency the situation of the maximum local SAR would get closer to the outer layer of the head. Also the results showed that the maximum SAR (10 g) was about 20% to 30% lower than maximum SAR (1 g) under similar conditions.

In conclusion, the important parameters affecting the absorbed energy in the human head exposed to mobile phone radiation were the type of antenna, current distribution and the distance between head and antenna; and, head models used for simulation did not play any significant role in the calculations.

## REFERENCES

1. "IEEE standard for safety level with respect to human exposure to radio frequency field, 3 KHz to 300 KHz," *Tech. Rep. IEEE C95.1*, 1999.
2. Balzano, Q. and T. J. Manning, "Electromagnetic energy exposure of simulated users of portable cellular telephones," *IEEE Trans.*, Vol. 44, 390–403, Aug. 1995.
3. Stavroulakis, P., *Biological Effects of Electromagnetic Fields*, Springer, 2002.
4. Hombach, V., K. Meier, M. Burkhardt, E. Kastle, and N. Kuster, "The dependence of electromagnetic energy absorption upon human head modeling at 900 MHz," *IEEE Trans. Microwave Theory Tech.*, Vol. 44, 1865–1873, Oct. 1996.
5. Hombach, V., K. Meier, M. Burkhardt, E. Kastle, and N. Kuster, "The dependence of electromagnetic energy absorption upon human head modeling at 1800 MHz," *IEEE Trans. Microwave Theory Tech.*, Vol. 45, 2058–2062, Nov. 1997.
6. Tinniswood, A. D. and O. P. Gandhi, "Computations of SAR distributions for two anatomically based models of the human head using CAD files of commercial telephones and the parallelized FDTD code," *IEEE Trans. Ant.*, Vol. 46, 829–833, 1998.
7. Dimbylow, P. J. and S. M. Mann, "SAR calculations in a anatomically realistic model of the head for mobile communication transceivers at 900 MHz and 1.8 GHz," *Physic in Medicine and Biology*, Vol. 39, 1537–1553, 1994.
8. Watanabe, S., M. Taki, T. Nojimi, and O. Fujiware, "Characteristics of the SAR distributions in a head exposed to electromagnetic fields radiated by a handheld portable radio," *IEEE Trans. Microwave*, Vol. 44, 1874–1883, 1996.
9. Taflove, A., *Advances in Computational Electromagnetics: The Finite Difference Time Domain Method*, Artech House, 1998.
10. Kunz, K. S. and R. J. Luebbers, *The Finite Difference Time Domain Method for Electromagnetics*, CRC Press, 1993.
11. Balanis, C. A., *Advanced Engineering Electromagnetics*, John Willy and Sons, New York, 1989.
12. Volakis, J., A. Chatterjee, and L. C. Kempel, *Finite Element Method for Electromagnetics*, IEEE Press, 1998.
13. Enguist, B. and A. Majda, "Absorbing boundary conditions for the numerical simulation of waves," *IEEE Trans. Electromagnetic*, Vol. 23, 377–382, Nov. 1987.
14. Chew, W. and J. Lin, "Perfectly matched layers in the discretized space," *IEEE Trans. Electromagnetics*, Vol. 16, 325–340, 1996.
15. Gandhi, O. P., G. Lazzi, and C. M. Furse, "Electromagnetic absorption in the human head and neck for mobile telephones at 835 and 1900 MHz," *IEEE Trans. Microwave*, Vol. 44, 1884–1897, 1996.

# Total Body Water Measured by Electromagnetic Resonant Cavity Perturbation

**D. A. Stone and M. P. Robinson**  
University of York, UK

**B. Oldroyd and J. Truscott**  
University of Leeds, UK

**A. Wright**  
MRC Human Nutritional Centre, UK

We recently demonstrated a novel method for determining human total body water (TBW) intended for patients suffering abnormal hydration using an electromagnetic resonant cavity perturbation (RCP) approach [1]. RCP relies on asking a volunteer to lie in a large cavity resonator and changes in its resonant frequency,  $f_{res}$ , are observed due to the consequent perturbation of the dielectric properties. Utilising the relationship that water content correlates to these dielectric properties at radio frequencies, it has been shown that the measured response of these parameters enables determination of body water [2]. Measurements are made using an automated network analyser operating in the transmission mode (measuring  $S_{21}$  or  $S_{12}$ ). The sensitivity can be demonstrated by asking a volunteer to drink a small amount of liquid between measurements, and is better than one litre. Although the sensitivity varies from subject to subject, we have shown that by fitting a second-order polynomial to the variation of the gradient versus the mass-to-height ratio, we are able to develop a prediction equation applicable to a wide range of ages and body types. Moreover, we have validated these equations by conducting a cross-validation study using three reference methods; our predictions of TBW have been shown to compare favourably.

**Method:** A rectangular electromagnetic screened room is utilised as an R.F cavity, which resonates at 59 MHz when energy is coupled into the room. Two monopole probes are mounted on the ceiling of the room and couple to the required vertical E-field ( $TE_{101}$  mode). Twenty-nine healthy volunteers were recruited and asked to lie in the centre of a screened room at York University, UK, before and after drinking 1.25–2 litres of water and isotonic fluid. For the cross-validation study, a further eighteen volunteers were invited to participate in a series of experiments at the Centre for Bone and Body Composition at the Leeds General Infirmary, UK. TBW for each volunteer was measured using three existing techniques; isotope dilution, dual X-ray absorptiometry and bio-impedance analysis. These volunteers were also measured in the screened room at York University.

**Results:** A combination of the isotope dilution data and the corresponding measurements of  $\Delta f_{res}$  taken in the screened room at York have been used to cross-validate the RCP prediction equations. Although a Bland and Altman plot was used to correct a -2litre drift in the data, agreement between the results is highly significant ( $r = 0.95$ ,  $p < 0.001$ ). Precision is also encouraging; the standard deviation of 37 paired measurements is 2.6 KHz, whilst resolution for the validation group ranges from 350–800 ml.

**Conclusions:** Predictions of TBW using electromagnetic RCP are favourable compared with reference methods; data is accurate and repeatable, and furthermore, resolution is better than 1 litre. This leads to confidence in the integrity of the proposed technique.

## REFERENCES

1. Robinson, M. P., J. Clegg, and D. A. Stone, "A novel method of studying total body water using a resonant cavity: experiments & numerical simulation," *Medicine in Physics and Biology*, Vol. 48, 113–125, 2003.
2. Stone, D. A and M. P. Robinson, "2003 total body water measurements using resonant cavity perturbation techniques," *Medicine in Physics and Biology*, Vol. 49, 1773–1788, 2004.

## **Influence of Electric Field Variation on Intracellular K<sup>+</sup> Ion Variations and Its Implication on Electrochemical Treatment**

**H. B. Kim<sup>1</sup>, S. B. Sim<sup>2</sup>, S. Y. Ahn<sup>1,3</sup>, W. Chang<sup>4</sup>, J.-H. Li<sup>4</sup>, and Y.-L. Xin<sup>4</sup>**

<sup>1</sup>Solco Biomedical Institute, Korea

<sup>2</sup>Catholic University, Korea

<sup>3</sup>Coll. Nat. Sci. of Seoul National University, Korea

<sup>4</sup>China-Japan Hospitality Hospital, China

Electrochemical Treatment(EchT) has been applied clinically to patients with diseases of hemangioma, lung and liver tumors, and so on.

In EchT, high electric field induces damage in the cells, first on the membrane than any other cell organelles due to higher resistance of the phospholipid bilayers in the cell. The field-induced voltage drop mainly occurs on the membrane. Moreover, because the cell dimension is a few orders of magnitude larger than the thickness of the cell membrane, the strength of the induced electric field within the membrane is hundred to thousand times higher than the apparent strength of the applied field. Such electric field may result in damage of the membrane phospholipid bilayer and membrane proteins, and thus change the potential of voltage-gated ion channels, especially potassium channels. In this study, we present the study on the variation of intracellular potassium ions via the confocal microscopy, and by increasing the strength of applied electric field from 5 V and up between two electrodes 5 mm apart.

# Qualitative Analysis of Human Semen Using Microwaves

A. Lonappan, A. V. Praveen Kumar, G. Bindu, V. Thomas, and K. T. Mathew  
Cochin University of Science and Technology, India

**Abstract**—Microwave engineering now a days plays a vital tool in diagnostic and therapeutic medicine. A quality evaluation of human semen at microwave frequencies using the measurements made at different intervals of time by cavity perturbation technique in the S-band of microwave spectrum is presented in this paper. Semen samples were also examined in the microscopic as well as macroscopic level in clinical laboratory. It is observed that conductivity of semen depends upon the motility of sperm and it increases as time elapses, which finds applications in forensic medicine.

## 1. Introduction

Accurate information about the dielectric properties of tissues and biological liquids is important for studies on the biological effects at radio and microwaves frequencies. In macroscopic level, these electrical properties determine the energy deposition patterns in tissue upon irradiation by an electromagnetic field. In microscopic level, they reflect the molecular mechanisms, which underlie the absorption of electromagnetic energy by the tissue or liquids. Knowledge of the microwave dielectric properties of human tissues is essential for the understanding and development of medical microwave techniques. Microwave thermography, microwave hyperthermia and microwave tomography all rely on processes fundamentally determined by the high frequency electromagnetic properties of human tissues. Tissue temperature pattern retrieval in the microwave thermography is achieved using models of the underlying tissue structure, which depend particularly on the dielectric properties of the tissue [1]. A recent review of published data on animal and human dielectric parameters shows that for most tissue types animal measurements are good substitute for human tissues [2].

Gabriel et al., Cook and Land et al., reported the dielectric parameters of various human tissues at different RF frequencies. [3–6]. Microwave study of human blood using coaxial line and wave-guide methods was carried out by Cook [7]. Tissue samples of human brain at microwave frequencies were analysed using sample cell terminated transmission line methods [8]. Open-ended coaxial line method allows measurements of tissue samples over a wide range of frequencies [9].

Microwave medical tomography is emerging as a novel non-hazardous method of imaging for the detection of fracture, swelling and diagnosis of tumors. Active and passive microwave imaging for disease detection and treatment monitoring require proper knowledge of body tissue dielectric properties at the lower microwave frequencies [10–12]. Studies on the variation of dielectric properties of body fluids and urinary calcifications at microwave frequencies have revealed that diagnosis is possible through cavity perturbation technique [13–15]. The present paper reports dielectric properties of semen at microwave frequencies as well as the quantitative analysis in the clinical laboratory. It is observed that conductivity of semen depends upon the motility of sperm as well as the time elapses after ejaculation.

## 2. Materials and Methods

The experimental set-up consists of a transmission type S-band rectangular cavity resonator, HP 8714 ET network analyser. The cavity resonator is a transmission line with one or both ends closed. The resonant frequencies are determined by the length of the resonator. The resonator in this set-up is excited in the  $TE_{10\rho}$  mode. The sample holder which is made of glass in the form of a capillary tube flared to a disk shaped bulb at the bottom is placed into the cavity through the non-radiating cavity slot, at broader side of the cavity which can facilitate the easy movement of the holder. The resonant frequency  $f_o$  and the corresponding quality factor  $Q_o$  of the cavity at each resonant peak with the empty sample holder placed at the maximum electric field are noted. The same holder filled with known amount of sample under study is again introduced into the cavity resonator through the non-radiating slot. The resonant frequencies of the sample loaded cavity is selected and the position of the sample is adjusted for maximum perturbation (i.e., maximum shift of resonant frequency with minimum amplitude for the peak). The new resonant frequency  $f_s$  and the quality factor  $Q_s$  are noted. The same procedure is repeated for other resonant frequencies.

### 3. Theory of Cavity Perturbation

When a material is introduced into a resonant cavity, the cavity field distribution and resonant frequency are changed which depend on shape, electromagnetic properties and its position in the fields of the cavity. Dielectric material interacts only with electric field in the cavity.

According to the theory of cavity perturbation, the complex frequency shift is related as [16]

$$-\frac{d\Omega}{\Omega} \approx \frac{(\bar{\epsilon}_r - 1) \int_{V_s} E \cdot E_0^* dV}{2 \int_{V_c} |E_0|^2 dV} \quad (1)$$

But

$$\frac{d\Omega}{\Omega} \approx \frac{d\omega}{\omega} + \frac{j}{2} \left[ \frac{1}{Q_s} - \frac{1}{Q_0} \right] \quad (2)$$

Equating (1) and (2) and separating real and imaginary parts results

$$\epsilon'_r - 1 = \frac{f_o - f_s}{2f_s} \left( \frac{V_c}{V_s} \right) \quad (3)$$

$$\epsilon''_r = \frac{V_c}{4V_s} \left( \frac{Q_o - Q_s}{Q_o Q_s} \right) \quad (4)$$

Here,  $\bar{\epsilon}_r = \epsilon'_r - j\epsilon''_r$ ,  $\bar{\epsilon}_r$  is the relative complex permittivity of the sample,  $\epsilon'_r$  is the real part of the relative complex permittivity, which is known as dielectric constant.  $\epsilon''_r$  is the imaginary part of the relative complex permittivity associated with the dielectric loss of the material.  $V_s$  and  $V_c$  are corresponding volumes of the sample and the cavity resonator. The conductivity can be related to the imaginary part of the complex dielectric constant as

$$\sigma_\epsilon = \omega\epsilon'' = 2\pi f\epsilon_0\epsilon''_r \quad (5)$$

### 4. Results and Discussion

Table 1: Variation of dielectric constant with frequency at different time intervals.

Frequency (MHz)	T = 5 minutes			
	M23	M24	M29	M33
2439.019	11.93	12.90	11.17	14.11
2683.882	11.91	12.44	10.93	12.52
2969.983	12.12	13.92	11.96	13.21
T = 15 minutes				
2439.019	12.73	12.97	11.21	13.12
2683.882	11.87	12.76	12.53	11.77
2969.983	11.77	13.01	10.11	12.23
T = 30 minutes				
2439.019	11.01	12.60	12.86	14.01
2683.882	12.37	12.56	12.38	13.81
2969.983	13.53	12.90	12.71	13.92
T = 45 minutes				
2439.019	13.31	12.61	11.74	13.22
2683.882	13.80	12.11	11.82	13.71
2969.983	13.06	12.84	11.95	13.51

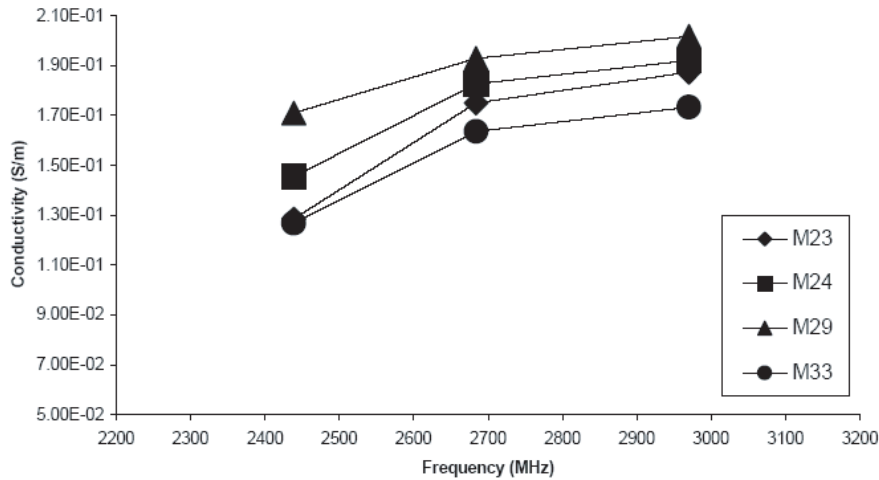


Figure 1: Conductivity of semen.

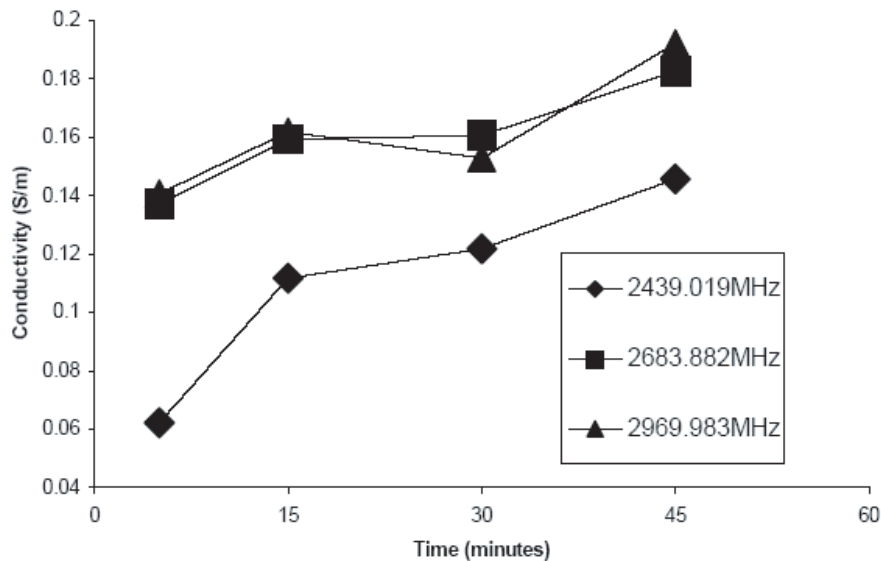


Figure 2: Temporal behaviour of conductivity of M24.

The microwave studies on the samples are done by cavity perturbation technique and the results are shown in Table 1 and in Figures 1 and 2. The clinical evaluation of the semen samples are done and the results are tabulated in Table 2. Table 1 indicates the variation of dielectric constant of different semen samples at different time intervals after ejaculation. It is observed that the dielectric constant is consistent at all frequencies at different intervals of time after ejaculation. From Figure 1, it is observed that the conductivity of the semen samples increases as frequency increases. This indicates that semen is lossier at higher frequencies due to the presence of the high motile quick sperms and its absorption of electromagnetic energy. The conductivity of the sample is more for high motile quick sperms and low conductivity for the dead sperms. From Figure 2, it is observed that the conductivity of semen increase as time elapses. This is due to the clotting enzyme of the prostatic fluid, which forms a coagulum in early stages after ejaculation, which makes the sperm remain relatively immobile, because of the viscosity of the coagulum [17]. The conductivity is relatively low due to this effect in early stages. As coagulum dissolves during the next 5 to 15 minutes, sperms become highly motile, which causes an increase in the conductivity.

This has potential application in forensic medicine in that the elapsed time after ejaculation is directly related to the conductivity of semen.

Table 2: Quantitative analysis of semen in the clinical laboratory.

SEMEN ANALYSIS				
	M23	M24	M29	M33
Time of collection	12.00 PM	12.15 PM	12.30 PM	12.35 PM
Time of liquefaction	12.30 PM	12.45 PM	1.00 PM	1.05 PM
MACROSCOPIC EXAMINATION				
Volume	1 ml	1.5 ml	0.5 ml	1 ml
Colour	Opaque grey	Opaque grey	Opaque grey	Opaque grey
Viscosity	Normal	Normal	Normal	Normal
pH	8.0	8.0	8.0	8.0
Liquefaction	Within 30 minutes	Within 30 minutes	Within 30 minutes	Within 30 minutes
MICROSCOPIC EXAMINATION				
Motility				
Quick	55 %	60 %	70 %	45 %
Sluggish	15 %	15 %	10 %	15 %
Dead	30 %	25 %	20 %	40 %
Sperm count	85million/ml	95 million/ml	100 million/ml	75million/ml
Pus cells	2-3/hpf	2-4/hpf	1-2/hpf	1-2/hpf
Morphology				
Normal	85 %	90 %	88 %	89 %
Giant Head	3 %	2 %	3 %	3 %
Round head	4 %	4 %	2 %	2 %
Pin head	5 %	2 %	4 %	5 %
Double head	3 %	2 %	3 %	1 %

## 5. Conclusion

The microwave study of the semen samples is done using cavity perturbation technique. This technique requires very small volume of sample and it is particularly applicable to biological samples like semen. The study shows that the dielectric constant of given semen sample does not show appreciable variation with time or with frequency. But it is observed that the conductivity of the semen sample increases as frequency increases, which shows that semen is lossier at higher frequencies. Samples with high conductivity indicates the presence of more high motile quick sperms and low conductivity indicate the more dead sperms. The conductivity of semen increases as time elapses and this finds application in forensic medicine to find the elapsed time after ejaculation.

## Acknowledgement

Authors Anil Lonappan and G. Bindu thankfully acknowledge Council of Scientific and Industrial Research, Government of India for providing Senior Research Fellowship.

## REFERENCES

1. Brown, V. J., "Development of computer modelling techniques for microwave thermography," Ph.D. Thesis, University of Glasgow, 1989.

2. Campbell, A. M. "Measurements and analysis of the microwave dielectric properties of tissue," Ph.D. Thesis, University of Glasgow, 1990.
3. Gabriel, C., S. Gabriel, and E. Corthout, "The dielectric properties of biological tissues: I. Literature survey," *Physics Medicine Biology*, Vol. 41, 2231–2249, 1996.
4. Gabriel, S., R. W. Lau, and C. Gabriel, "The dielectric properties of biological tissues: II. Measurements on the frequency range 10 Hz to 20 GHz," "Literature survey," *Physics Medicine Biology*, Vol. 41, 2251–2269, 1996.
5. Cook, H. F., "The dielectric behavior of some types of human tissues at microwave frequencies," *British Journal of Applied Physics*, Vol. 2, 295–300, Oct. 1951.
6. Land, D. V. and A. M. Campbell, "A quick accurate method for measuring the microwave dielectric properties of small tissue samples," *Physics Medicine Biology*, Vol. 37, 183–192, 1992.
7. Cook, H. F., "Dielectric behavior of human blood at microwave frequencies," *Nature*, Vol. 168, 247–248, 1951.
8. Foster, K. R., J. L. Schepps, R. D. Stoy, and H. P. Schwan, "Dielectric properties of brain tissue between 0.01 and 10 GHz," *Phys. Med. Biol.*, Vol. 24, 1177–87, 1979.
9. Athey, T. W., M. A. Stuchly, and S. S. Stuchly, "Measurement of radio frequency of biological tissues with an open-ended coaxial line," *IEEE Trans. Microwave Theory Techn.*, Vol. 30, 82–86, 1982.
10. Bolomey, J. Ch., G. Perronnnet, and L. Jofre, "On the possible use of active microwave imaging for remote thermal sensing," *IEEE Trans. Microwave Theory Techn.*, Vol. 31, 777–781, 1983.
11. Broquetas, A., M. S. Hawley, and L. Jofre, "Active microwave computed tomography cylindrical scanner for biomedical application," *J. Photo. Sci.*, Vol. 37, 151–153, 1989.
12. Land, D. V., "A clinical microwave thermography system," *IEE Proc.*, Vol. 134A, 193–200, 1987.
13. Paul, I., G. Varghese, M. A. Ittyachen, K. T. Mathew, A. Lonappan, J. Jacob, and S. B. Kumar, "Dielectric properties of urinary stones at microwave frequencies," *Microwave and Optical Technology Letters (USA)*, Vol. 35, No. 4, 297–299, November 2002.
14. Kumar, S. B., K. T. Mathew, U. Raveendranath, and P. Augustine, "Dielectric properties of certain biological materials at microwave frequencies," *The Journal of Microwave Power & Electromagnetic Energy*, Vol. 36, No. 2, 67–75, 2001.
15. Lonappan, A., V. Hamsakutty, G. Bindu, J. Jacob, V. Thomas, and K. T. Mathew, "Dielectric properties of human urine at microwave frequencies," *Microwave and Optical Technology Letters (USA)*, Vol. 42, No. 6, 500–503, September 2004.
16. Mathew, K. T. and U. Raveendranath, "Sensors update," Wiley-VCH, Germany, Vol. 7, 185, 1999.
17. Guyton, A. C., *Textbook of medical physiology*, 8<sup>th</sup> Edition, Prism Books Pvt. Ltd.

## Microwave Thermotherapy — Technical and Clinical Aspects

J. Vrba, L. Oppl, J. H. Trefna, T. Drizdal, and R. Zajicek

Czech Technical University, Czech Republic

J. Kvěch and J. Kubeš

Institute of Radiation Oncology, Czech Republic

We would like to describe our new technical results dealing with microwave thermotherapy in the cancer treatment. Our research interest is to develop applicators for deep local heating and for intracavitary cancer treatment as well. Basic evaluation of clinical results is presented.

### Deep Local and Regional Applicators

Microwave thermotherapy (hyperthermia) is being used for cancer treatment since early 80's in many countries around the world. Since 1981 we were interested in the local external applicators working at 434 MHz and 2450 MHz. These applicators were used here in Prague for the treatment of more than 500 patients with superficial or subcutaneous tumours (up to the depth of approximately 4 cm). Now, following new trends in this field, we continue our research in two important directions:

- deep local and regional applicators,
- intracavitary applicators.

For the deep local thermotherapy treatment we develop above all waveguide type applicators based on the principle of evanescent mode waveguide, which is our specific solution and original contribution to the theory of microwave hyperthermia applicators. This technology enable us:

- to design applicators with as small aperture as necessary also for the optimum frequency range for deep local and/or for regional thermotherapy treatment (the frequency band between 27 and 70 MHz).
- using our technology we need not to fill the applicator by dielectric (necessary for deep penetration into the biological tissue - i.e., up to 10 centimetres under the body surface).
- two to four of such applicators can be also used for regional treatment.

Waveguide type applicators are often used in the local external hyperthermia treatment of cancer and other modifications of microwave thermotherapy as they offer very advantageous properties, above all:

- depth of penetration of the EM energy approaching the ideal case of plane wave,
- low irradiation of the energy in the vicinity of the hyperthermia apparatus,
- very good impedance matching, i.e., perfect energy transfer to the biological tissue.

We have studied waveguide applicators heating pattern for the aperture excitation at above and at under the cutoff frequency. It has helped us to get analytical approximations of the electromagnetic field distribution in the treated area of the biological tissue. The most important results for the effective heating depth  $d$  can be characterised as follows:

- at high frequencies (above approx. 1000 MHz) the depth of effective heating  $d$  is above all a function of frequency  $f$  (skin effect),
- below approx. 100 MHz  $d$  is the dominantly function of the diameter  $D$  of applicator aperture ( $d = 0.386D$ ).

### Clinical Results

In the case of cancer treatment the long term statistics of clinical results can be described as follows:

- Complete Response of Tumor .....53%
- Partial Response of the Tumor ...31%
- No Significant Response .....16%

which corresponds to results obtained also by other groups in Europe.

\*This research is supported by Grant Agency of the Czech Republic, project: "Microwave Imaging for Biomedical Applications" (102/05/0959) and by the research program MSM6840770012 "Transdisciplinary Research in the Area of Biomedical Engineering II" of the CTU in Prague, sponsored by the Ministry of Education, Youth and Sports of the Czech Republic.

## Relative Absorption of Electromagnetic Energy in Adjacent Tissues

Y. V. Narayana<sup>1</sup>, G. N. Devi<sup>2</sup>, and G. S. N. Raju<sup>3</sup>

<sup>1</sup>ANITS Engineering College, India

<sup>2</sup>55-1-26, J.R. Nagar, Venkojipalem, India

<sup>3</sup>AU College of Engineering, India

The hyperthermia is an effective form of therapy over the years. In this technique, the elevated temperatures are used for the treatment. It is possible to make use of the heat generated as a result of raise in temperature for effectively treating the tumors and cancerous tissues. This is possible by allowing electromagnetic energy to incident on the effective tissues for defined intervals.

For effective applications of such methods, the knowledge of the electromagnetic energy absorption in different biological tissues is required. In fact, the absorption depends on frequency and the characteristics of the tissues.

In the present work, some studies are made to evaluate the relative absorption of electromagnetic energy for different pairs of adjacent tissues. It is well known that, the permittivity, conductivity are also functions of frequency and they differ from tissue to tissue.

The different orientations of the electric field of the electromagnetic wave are considered for computing the above mentioned data. From the data obtained in the present work, the relative absorption of electromagnetic energy is found to vary for each pair of tissues. It is also found to be dependent on the polarizations of the electromagnetic wave that is incident on the tissues. The data of the present work is useful for the design of radiation sources.

## Detection and Identification of Bio-medical Materials Possessing Chirality Using the Mueller Matrix

**E. Bahar**

University of Nebraska-Lincoln, USA

Since bio-medical materials possess some degree of chirality, the specific impact of chirality on the Mueller Matrix elements is analyzed. The canonical solutions for electromagnetic propagation in chiral media are the right and left circular polarized waves. Therefore, initially the effects of chirality on the circular like and cross polarized reflection coefficients are obtained.

It is shown that to within first order in the chirality parameters, only the circular, like polarized reflection coefficients (right to right, left to left) are modified. However since the Mueller Matrix elements are usually expressed in terms of linear like and cross polarized scattering coefficients, the corresponding expressions for the linear polarized reflection coefficients are determined. It is shown that only the linear, cross polarized reflection coefficient are modified. As a result (to within first order in the chirality parameter) only the eight quasi off diagonal elements of the Mueller Matrix are effected by the chiral property of the bio-medical materials. This reinforces the experimental observations from previous scattering experiments that the quasi off diagonal Mueller Matrix elements could provide a basis for detection and identification of bio-medical materials.

The analysis provides the explicit relationship between the quasi off diagonal elements and the degree of chirality of the bio-medical material. Thus it is possible to determine whether the chiral effects are sufficiently large to provide the accuracy necessary to conduct species-level discrimination in the present of spurious contributions due to surface roughness, etc. The explicit dependence of the Mueller Matrix elements (due to chirality) upon frequency and angles of incidence is also determined. Thus it is possible to optimize the impact of chirality on the Mueller Matrix in order to improve the feasibility of species level discrimination.

## Co-design Planar Antenna for “UWB”

**T.-P. Vuong, Y. Duroc, and S. Tedjini**  
 Institute National Polytechnique de Grenoble, France

**G. Fontgalland**  
 LEMA de l'Universidade Federal de Campina Grande, Brazil

In this paper a wide band antenna to cover the UWB band is proposed. One of the main features of this antenna is the rejection frequency in the Wi-Fi band (around 5.2 GHz). The analysis results of the antennas parameters,  $S_{11}$ , VSWR and the radiated pattern, are presented. The communications, in special wireless, are in the top of attention of researchers. The need of a high velocity bit transmission rate and the great number of services that restrict the free operation band ask for new solutions to the communications systems. The UWB (Ultra Wide Band) technology seems to be very prominent for this application, since it operates in a large band with very low power transmission. The antenna in the UWB applications plays an important role. This is the reason why it is in focus. In this study for a new antenna, before goes to step measurement, a commercial electromagnetic software CST microwave Studio version 5.0 is used to simulate antennas parameters. The antenna geometry was simulated using a dielectric with relative permittivity  $\epsilon_r = 4.4$ . The geometry obtained here is optimized to reduce antenna dimensions. The co-design antenna (Fig. 1) presents the behavior of a classical large band antenna and the behavior of a rejection band structure. In our case, the rejection is selected to be around the Wi-Fi band (5.2 GHz). From Fig. 2, we can see that the new proposed antenna works with reflection coefficient below of -10 dB in the band of 3.1 to 4.75 GHz and from 5.6 to 13.2 GHz.

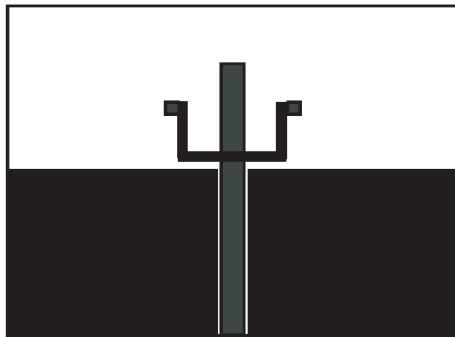


Figure 1: Co-design of studied patch antenna.

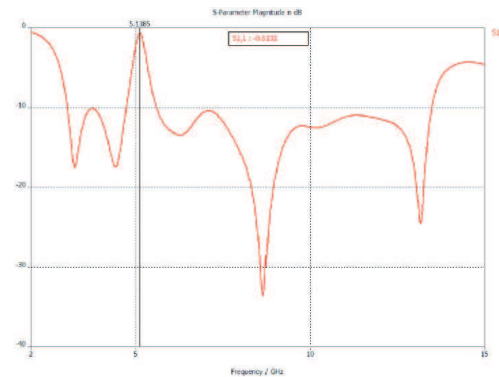


Figure 2: Parameter  $S_{11}$  of the UWB antenna.

